Reactivity of $[NBu_4][(C_6F_5)_2M(\mu\text{-}PPh_2)_2M'(acac\text{-}O,O')]$ (M, M′ = Pt, Pd) toward Silver Centers. Synthesis of Polynuclear Complexes Containing M−Ag Bonds (M = Pd, Pt)†

Ester Alonso,‡ Juan Forniés,*,‡ Consuelo Fortuño,‡ Antonio Martín,‡,§ and A. Guy Orpen§

Departamento de Química Inorgánica and Instituto de Ciencia de Materiales de Aragón, Universidad de Zaragoza-CSIC, 50009 Zaragoza, Spain, and School of Chemistry, University of Bristol, Cantocks Close, Bristol BS8 ITS, U.K.

Received July 17, 2003

The binuclear complexes $[NBu_4][(C_6F_5)_2M(\mu\text{-}PPh_2)_2M'(acac\text{-}O,O')]$ (M = M′ = Pt, **1a**; M = Pt, M′ = Pd, **1b**; M = M′ = Pd, **1c**) have been prepared by reacting $[NBu_4]_2[(C_6F_5)_2M(\mu\text{-}PPh_2)_2M'(\mu\text{-}Cl)_2M'(\mu\text{-}PPh_2)_2M(C_6F_5)_2]$ with Tl(acac). Complexes **1a**,**b** react with $[Ag(OClO_3)(PPh_3)]$, yielding $[MPtAg(\mu\text{-}PPh_2)_2(C_6F_5)_2(acac)(PPh_3)]$ (M = Pt**, 2a**; M = Pd, **2b**). The X-ray structures of both complexes are rather similar, the main difference being related with the Pt−Ag bonds. While in **2b** it is clear that there are Pt−Ag and Pd−Ag bonds, in **2a** it seems that only one Pt−Ag bond is connecting both Pt and $AgPPh_3$ moieties. The formation of a Pd−Ag bond is rather surprising, because of the known reluctance of the Pd center to engage in this sort of bonding. **1a**,**b** react with equimolar amounts of $AgClO_4$ in CH_2Cl_2 to give $[PtMAg(\mu\text{-}PPh_2)_2(C_6F_5)_2(acac)]_x$ (M = Pt, **4a**; M = Pd, **4b**). The X-ray structure of **4a** indicates that the "$Pt_2(acac)(C_6F_5)_2(\mu\text{-}PPh_2)$" fragments are connected to the silver center through two Pt−Ag bonds (2.875(1), 2.864(1) Å) and one C^{γ}−Ag bond (of the acac ligand). On the other hand, when the homodinuclear palladium derivative reacts with $[Ag(OClO_3)(PPh_3)]$ or $AgClO_4$, decomposition takes place and $[(C_6F_5)(PPh_3)Pd(\mu\text{-}PPh_2)_2Pd(acac)]$ can be detected in the former reaction. These processes are in agreement with the well-known tendency of the pentafluorophenyl−palladate substrates to participate in arylating processes.

Introduction

Earlier work in our laboratory has established that anionic (perhalophenyl)platinate complexes behave as Lewis bases and react with silver derivatives to afford polynuclear complexes displaying donor−acceptor Pt−Ag bonds.[1] As far as the dinuclear platinate complexes are concerned, in cases such as $[NBu_4]_2[(C_6F_5)_2Pt(\mu\text{-}X)_2Pt(C_6F_5)_2]$ (X = Cl, C_6F_5) they react with silver derivatives, yielding the trinuclear complexes $[NBu_4][Pt_2Ag(\mu\text{-}X)_2(C_6F_5)_4L]$ (Scheme 1, type A) and acting as bidentate chelating ligands toward the silver center.[2−4] In a similar way the dinuclear complexes $[NBu_4][(C_6F_5)_2Pt(\mu\text{-dppm})(\mu\text{-}X)Pt(C_6F_5)_2]$ (X = Cl, Br, OH) react with $[Ag(OClO_3)L]$, forming trinuclear derivatives with two Pt−Ag bonds (donor−acceptor bonds).[5]

Scheme 1

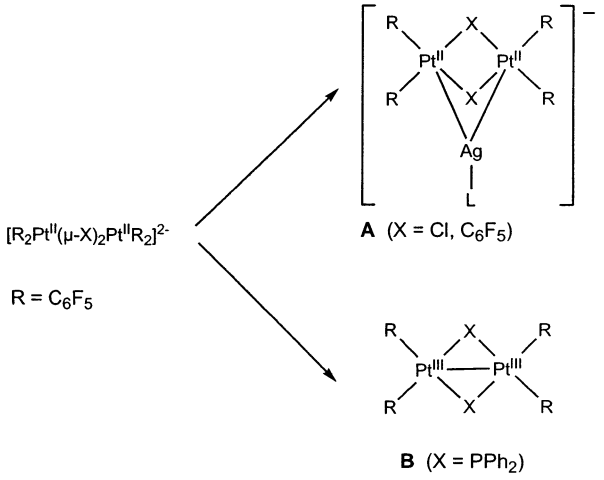

To our surprise, the reactions of the di- and trinuclear phosphido complexes $[NBu_4]_2[Pt_2(\mu\text{-}PPh_2)_2(C_6F_5)_4]$ and $[NBu_4]_2[Pt_3(\mu\text{-}PPh_2)_4(C_6F_5)_4]$ with $AgClO_4$ result in the formation of Ag(0) and platinum complexes with Pt in an oxidation state higher than II, $[(C_6F_5)_2Pt(\mu\text{-}PPh_2)_2Pt(C_6F_5)_2]$[6] (Scheme 1, type B) and $[(C_6F_5)_2Pt(\mu\text{-}PPh_2)_2Pt(\mu\text{-}PPh_2)_2Pt(C_6F_5)_2]$,[7] but not in complexes with Pt−Ag bonds.

† Polynuclear Homo- or Heterometallic Palladium(II)-Platinum(II) Pentafluorophenyl Complexes Containing Bridging Diphenylphosphido Ligands. 13. Part 12: ref 34.

‡ Universidad de Zaragoza-CSIC.

§ University of Bristol.

(1) Forniés, J.; Martín, A. In *Metal Clusters in Chemistry*; Braunstein, P., Oro, L. A., Raithby, P. R., Eds.; Wiley-VCH: Weinheim, Germany, 1999; Vol. 1, pp 417−443.

(2) Usón, R.; Forniés, J.; Tomás, M.; Casas, J. M.; Cotton, F. A.; Falvello, L. R. *Inorg. Chem.* **1987**, *26*, 3482−3486.

(3) Usón, R.; Forniés, J.; Tomás, M.; Casas, J. M.; Cotton, F. A.; Falvello, L. R.; Llusar, R. *Organometallics* **1988**, *7*, 2279−2285.

(4) Casas, J. M.; Forniés, J.; Martín, A.; Menjón, B.; Tomás, M. *Polyhedron* **1996**, *15*, 3599−3604.

(5) Casas, J. M.; Falvello, L. R.; Forniés, J.; Martín, A. *Inorg. Chem.* **1996**, *35*, 7867−7872.

10.1021/om034047f CCC: $25.00
Publication on Web 10/28/2003

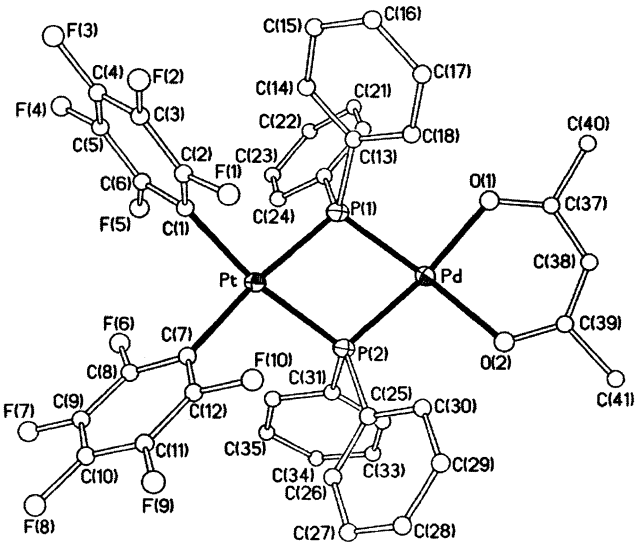

Figure 1. Structure of the complex anion of $[NBu_4][PtPd(\mu\text{-}PPh_2)_2(C_6F_5)_2(acac)]$ (**1b**).

Since, in our experience, the ability of the platinate substrates to act as Lewis bases toward silver salts is strongly dependent on the nature of the ancillary ligands bonded to platinum,[1] we have synthesized other binuclear M/M′ (M, M′ = Pd, Pt) phosphido complexes such as $[NBu_4][(C_6F_5)_2M(\mu\text{-}PPh_2)_2M'(acac)]$ and studied their reactivity toward $[Ag(OClO_3)(PPh_3)]$ and $AgClO_4$. The results of these reactions are reported in this paper.

Results and Discussion

Synthesis of $[NBu_4][(C_6F_5)_2M(\mu\text{-}PPh_2)_2M'(acac\text{-}O,O')]$ (M = M′ = Pt, 1a; M = Pt, M′ = Pd, 1b; M = M′ = Pd, 1c). The reaction of $[NBu_4]_2[(C_6F_5)_2M(\mu\text{-}PPh_2)_2M'(\mu\text{-}Cl)_2M'(\mu\text{-}PPh_2)_2M(C_6F_5)_2]$ with Tl(acac) (1:2 molar ratio) in CH_2Cl_2 at room temperature results in the precipitation of TlCl and formation of $[NBu_4][(C_6F_5)_2M(\mu\text{-}PPh_2)_2M'(acac\text{-}O,O')]$ (M = M′ = Pt, **1a**; M = Pt, M′ = Pd, **1b**; M = M′ = Pd, **1c**).

The structure of **1b** has been determined by an X-ray diffraction study. The structure of the anion of complex **1b** together with the atom-labeling scheme is shown in Figure 1. Selected bond distances and angles are listed in Table 1. Complex **1b** is a dinuclear complex in which the metal centers are bridged by two diphenylphosphido ligands. The environments of both metal atoms are typically square planar, the dihedral angle between the two best square planes being 16.0(1)°. The long intermetallic distance, 3.555(1) Å, precludes any kind of Pt···Pd interaction. In accordance with this observation, the Pt−P−Pd angles are large (103.49(3) and 102.57(3)°, respectively). The geometry observed around the palladium atom is very similar to that reported for the complex $[Pd_2(\mu\text{-}PPh_2)_2(F_6acac\text{-}O,O')_2]$,[8] a symmetrical dinuclear complex which also contains PPh_2 bridging ligands. Thus, for **1b** the Pd−O distances are 2.083(2) and 2.105(2) Å and the O−Pd−O angle is 90.07(9)°,

Table 1. Selected Bond Distances (Å) and Angles (deg) for $[NBu_4][PtPd(\mu\text{-}PPh_2)_2(C_6F_5)_2(acac)]\cdot Me_2CO$ ($1b\cdot Me_2CO$)

Pt-C(1)	2.064(3)	Pd−O(1)	2.083(2)
Pt−P(2)	2.3006(8)	Pd−P(2)	2.2594(9)
Pd−P(1)	2.2459(9)	Pt−P(1)	2.2852(9)
Pt−C(7)	2.075(3)	Pd−O(2)	2.105(2)
C(1)−Pt−C(7)	90.76(12)	C(1)−Pt−P(1)	95.09(9)
C(7)−Pt−P(1)	172.55(9)	C(1)−Pt−P(2)	170.03(9)
C(7)−Pt−P(2)	98.65(9)	P(1)−Pt−P(2)	75.27(3)
O(1)−Pd−O(2)	90.07(9)	O(1)−Pd−P(1)	94.84(7)
O(2)−Pd−P(1)	173.69(7)	O(1)−Pd−P(2)	171.63(7)
O(2)−Pd−P(2)	98.28(7)	P(1)−Pd−P(2)	76.85(3)
Pd−P(1)−Pt	103.49(3)	Pd−P(2)−Pt	102.57(3)

whereas in $[Pd_2(\mu\text{-}PPh_2)_2(F_6acac\text{-}O,O')_2]$ the Pd−O distances are 2.098(5) and 2.111(4) Å and the O−Pd−O angle is 88.8°. Also, for $[Pd_2(\mu\text{-}PPh_2)_2(F_6acac\text{-}O,O')_2]$ the intermetallic distance (3.565(1) Å) and the M−P−M angles (105.8(1)°) are similar to those found in **1b**, but the "$Pd_2(\mu\text{-}PPh_2)_2$" core is perfectly planar. In **1b**, the acac ligand has a planar configuration, forming a dihedral angle with the best Pd square plane of 12.1(1)°. In the case of $[Pd_2(\mu\text{-}PPh_2)_2(F_6acac\text{-}O,O')_2]$, the dihedral angle formed by the F_6acac ligand (which is also planar) with the best palladium square plane has a value of 6.8°.

The IR spectra of complexes **1a**−**c** show two bands at about 800 cm^{-1} (X-sensitive mode of the C_6F_5 groups),[9,10] in accordance with the presence of two mutually cis C_6F_5 groups, and characteristic absorptions at ca. 1580 and 1515 cm^{-1} due to the acac group (see the Experimental Section). The absorption due to the O,O′-coordinated acac group[11−13] at ca. 800 cm^{-1} cannot be unambiguously assigned, due to the presence in this region of bands of the X-sensitive mode of the C_6F_5 groups. The ^1H NMR spectra reveal for the acac group two singlets, one corresponding to the C$^{\gamma}H$ group and the other to the two equivalent CH_3 groups. The ^{19}F NMR spectra show three sets of signals corresponding to *o*-F, *m*-F, and *p*-F, respectively, indicating that the two C_6F_5 groups are equivalent, as are the halves of each ring. The $^{31}P\{^1H\}$ NMR spectra show one high-field signal, in accordance with the presence of two equivalent PPh_2 groups acting as bridging ligands between two metal centers not joined by a metal−metal bond.[7,14] It has been established that usually the chemical shift decreases as the atomic number increases from top to bottom in a triad.[15] In agreement with this, the chemical shifts from **1c** (Pd_2, −115.6 ppm) to **1b** (PdPt, −134.2 ppm) and to **1a** (Pt_2, −144.6 ppm) show that this P atom is shielded upon substitution of a palladium by a platinum center, as we have observed before.[7] From the platinum satellites two values of $^1J_{Pt-P}$ (1912 and

(6) Alonso, E.; Casas, J. M.; Cotton, F. A.; Feng, X. J.; Forniés, J.; Fortuño, C.; Tomás, M. *Inorg. Chem.* **1999**, *38*, 5034−5040.
(7) Alonso, E.; Casas, J. M.; Forniés, J.; Fortuño, C.; Martín, A.; Orpen, A. G.; Tsipis, C. A.; Tsipis, A. C. *Organometallics* **2001**, *20*, 5571−5582.
(8) Bekiaris, G.; Roschenthaler, G. V.; Behrens, U. *Z. Anorg. Allg. Chem.* **1992**, *618*, 153.
(9) Usón, R.; Forniés, J. *J. Adv. Organomet. Chem.* **1988**, *28*, 219−297.
(10) Maslowsky, E. J. *Vibrational Spectra of Organometallic Compounds*; Wiley: New York, 1997.
(11) Forniés, J.; Martínez, F.; Navarro, R.; Urriolabeitia, E. *Organometallics* **1996**, *15*, 1813−1819.
(12) Forniés, J.; Navarro, R.; Tomás, M.; Urriolabeitia, E. *Organometallics* **1993**, *12*, 940−943.
(13) Nakamoto, K. *Infrared and Raman Spectra of Inorganic and Coordination Compounds*, 4th ed.; Wiley-Interscience: New York, 1986.
(14) Alonso, E.; Forniés, J.; Fortuño, C.; Martín, A.; Orpen, A. G. *Organometallics* **2001**, *20*, 850−859.
(15) Carty, A. J.; MacLaughlin, S. A.; Nucciarone, D. *Phosphorus-31 NMR Spectroscopy in Stereochemical Analysis*; VCH: Weinheim, Germany, 1987.

Scheme 2[a]

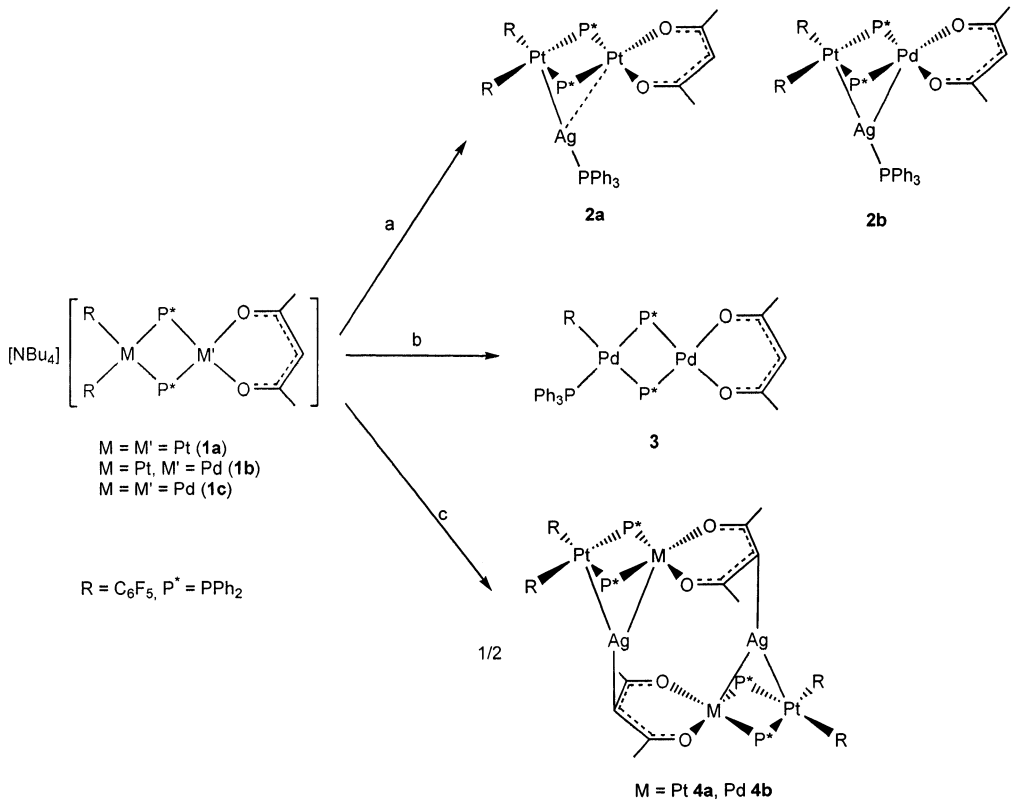

[a] Legend: (a) +[Ag(OClO$_3$)(PPh$_3$)], −NBu$_4$ClO$_4$; (b) +[Ag(OClO$_3$)(PPh$_3$)], −Ag(C$_6$F$_5$), −NBu$_4$ClO$_4$; (c) +AgClO$_4$, −NBu$_4$ClO$_4$.

2641 Hz) for **1a** and a value (1785 Hz) for **1b** can be extracted. The higher value in **1a** is assigned to the coupling with the platinum center bonded to the acac ligand. Relevant spectroscopic data for **1a**−**c** are given in the Experimental Section.

Reactions between [NBu$_4$][(C$_6$F$_5$)$_2$M(*μ*-PPh$_2$)$_2$M′-(acac-*O*,*O*′)] and [Ag(OClO$_3$)(PPh$_3$)] or AgClO$_4$. The reaction of [NBu$_4$][(C$_6$F$_5$)$_2$Pt(*μ*-PPh$_2$)$_2$M(acac)] (M = Pt, **1a**; M = Pd, **1b**) with an equimolar amount of [Ag(OClO$_3$)(PPh$_3$)] in CH$_2$Cl$_2$ at room temperature results in the formation of yellow solutions from which the trinuclear clusters [MPtAg(*μ*-PPh$_2$)$_2$(C$_6$F$_5$)$_2$(acac)(PPh$_3$)] (M = Pt**, 2a**; M = Pd, **2b**) are obtained (Scheme 2, path a).

The crystal structures of complexes **2a**,**b** have been determined by X-ray diffraction, and they are shown in Figures 2 and 3, respectively. Selected bond distances and angles are listed in Tables 2 and 3, respectively. The structures of the two complexes are very similar. For descriptive purposes, they can be regarded as the union of the dinuclear "(C$_6$F$_5$)$_2$Pt(*μ*-PPh$_2$)$_2$M(acac)" fragment with the "Ag(PPh$_3$)" moiety through only Pt− or Pd−Ag donor−acceptor bonds. In the first fragment the metal atoms are linked by two diphenylphosphido ligands, but their separation (Pt(1)−Pt(2) = 3.515(1) Å in **2a** and Pt−Pd = 3.478(1) Å in **2b**) allows us to exclude any kind of metal−metal bond. In both structures, the Pt and Pd atoms lie in typical square-planar environments, but the dinuclear "(C$_6$F$_5$)$_2$Pt(*μ*-PPh$_2$)$_2$M-(acac)" fragments are not planar. The dihedral angles between the best least-squares planes are 19.3(1)° for **2a** and 33.5(1)° for **2b** (compare with the value of this parameter, 16.0(1)°, in the starting material **1b**). The acac ligands are essentially planar and almost coplanar

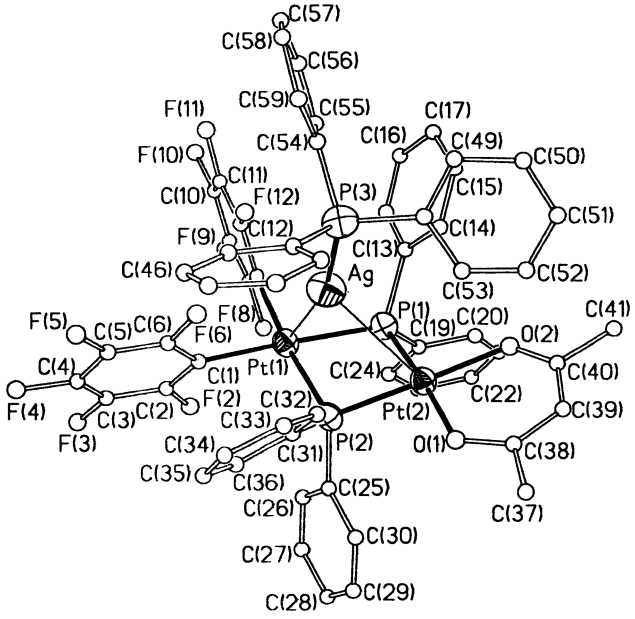

Figure 2. Structure of the complex [Pt$_2$Ag(*μ*-PPh$_2$)$_2$(C$_6$F$_5$)$_2$-(acac)(PPh$_3$)] (**2a**).

with the square-planar environment of Pt(2) (**2a**, the dihedral angle is 3.4(1)°) or Pd (**2b**, 5.7(1)°).

The Pt−Ag distances found in **2a** are rather different. While the Pt(1)−Ag distance is 2.793(1) Å, a value within the range found for Pt−Ag donor−acceptor bonds, the Pt(2)−Ag distance is somewhat long, 3.098(1) Å, for this kind of bond.[1,16] On the other hand, the Pt-(1)−Ag vector forms an angle with the perpendicular of the best least-squares Pt(1) plane of 21.3(1)°, while

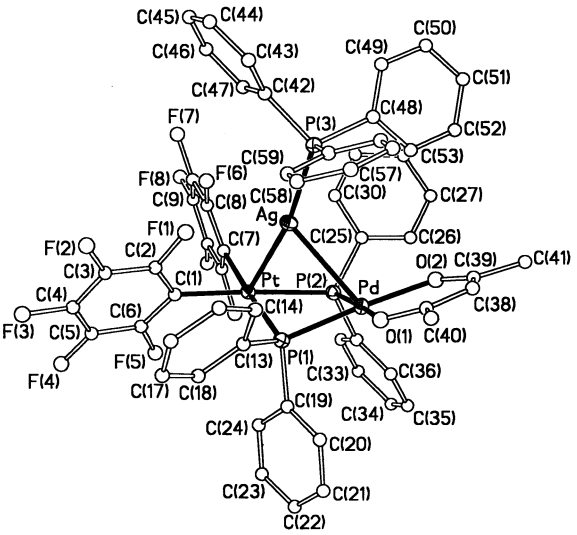

Figure 3. Structure of the complex $[PtPdAg(\mu\text{-}PPh_2)_2(C_6F_5)_2(acac)(PPh_3)]$ (**2b**).

Table 2. Selected Bond Distances (Å) and Angles (deg) for $[Pt_2Ag(\mu\text{-}PPh_2)_2(C_6F_5)_2(acac)(PPh_3)]\cdot CHCl_3$ (2a·$CHCl_3$)

Pt(1)−C(7)	2.072(8)	Pt(2)−P(1)	2.252(2)
Pt(1)−P(2)	2.324(2)	Ag−P(3)	2.392(2)
Pt(2)−O(1)	2.078(5)	Pt(1)−P(1)	2.317(2)
Pt(2)−Ag	3.098(1)	Pt(2)−O(2)	2.075(5)
Pt(1)−C(1)	2.087(9)	Pt(2)−P(2)	2.252(2)
Pt(1)−Ag	2.793(1)		
C(7)−Pt(1)−C(1)	87.5(3)	C(7)−Pt(1)−P(1)	98.3(2)
C(1)−Pt(1)−P(1)	172.5(3)	C(7)−Pt(1)−P(2)	174.3(2)
C(1)−Pt(1)−P(2)	97.8(2)	P(1)−Pt(1)−P(2)	76.3(1)
O(2)−Pt(2)−O(1)	89.5(2)	O(2)−Pt(2)−P(1)	94.7(2)
O(1)−Pt(2)−P(1)	175.6(2)	O(2)−Pt(2)−P(2)	172.6(2)
O(1)−Pt(2)−P(2)	96.7(2)	P(1)−Pt(2)−P(2)	79.0(1)
P(3)−Ag−Pt(1)	164.8(1)	P(3)−Ag−Pt(2)	122.0(1)
Pt(1)−Ag−Pt(2)	73.0(1)	Pt(2)−P(1)−Pt(1)	100.6(1)
Pt(2)−P(2)−Pt(1)	100.3(1)		

Table 3. Selected Bond Distances (Å) and Angles (deg) for $[PtPdAg(\mu\text{-}PPh_2)_2(C_6F_5)_2(acac)(PPh_3)]\cdot 2.5CH_2Cl_2$ (2b·$2.5CH_2Cl_2$)

Pt−C(1)	2.062(6)	Pd−P(1)	2.252(2)
Pt−P(2)	2.333(2)	Ag−P(3)	2.372(2)
Pd−O(2)	2.069(5)	Pt−P(1)	2.297(2)
Pd−Ag	2.886(1)	Pd−O(1)	2.065(5)
Pt−C(7)	2.085(7)	Pd−P(2)	2.274(2)
Pt−Ag	2.733(1)		
C(1)−Pt−C(7)	88.9(2)	C(1)−Pt−P(1)	94.16(17)
C(7)−Pt−P(1)	176.88(19)	C(1)−Pt−P(2)	167.37(18)
C(7)−Pt−P(2)	102.65(18)	P(1)−Pt−P(2)	74.23(6)
O(1)−Pd−O(2)	90.26(19)	O(1)−Pd−P(1)	98.08(14)
O(2)−Pd−P(1)	170.24(14)	O(1)−Pd−P(2)	173.56(14)
O(2)−Pd−P(2)	95.67(14)	P(1)−Pd−P(2)	76.25(7)
P(3)−Ag−Pt	166.26(5)	P(3)−Ag−Pd	116.02(5)
Pt−Ag−Pd	76.43(2)	Pd−P(1)−Pt	99.74(7)
Pd−P(2)−Pt	98.02(7)		

the Pt(2)−Ag vector forms an angle of 32.4(1)° with the perpendicular of the best least-squares Pt(2) plane. It is now well established that, for this kind of complex, the stronger Pt−Ag bonds are achieved when these bonds are nearer to perpendicular to the platinum square coordination plane[1] and that the dinuclear platinate substrates which act as bidentate ligands to the M centers adopt an "open book" disposition in order to favor the formation of the two Pt−M bonds as close as possible to perpendicular. In this way a better overlap between the filled $5d_{z^2}$ platinum orbital and the empty orbitals of the Lewis acidic M center can be achieved.[2−5]

When these facts are taken into account, it can be concluded that in **2a** there is only a Pt(1)−Ag donor−acceptor bond and that Pt(2) is only weakly interacting (if at all) with the Ag center.

The M−Ag distances in complex **2b** are rather surprising. The Pt−Ag distance, 2.733(1) Å, is similar to the analogous length in **2a**, but the Pd−Ag distance, 2.886(1) Å, is ca. 0.21 Å shorter than the Pt(2)−Ag distance in **2a**. Also, while in **2b** the Pt−Ag vector forms an angle of 18.8(1)° with the perpendicular of the best square platinum coordination plane, a value similar to the analogous value in **2a,** the corresponding angle involving the Pd atom is 24.3(1)°, significantly less than the analogous value in **2a,** 32.4(1)°. As mentioned above, the dihedral angle between the two square planes of the complex is larger for **2a** than for **2b** and, thus, the "book is more closed" in the latter. All these geometrical observations for **2b** (i.e. the shorter Pd−Ag distance, the more nearly perpendicular Pd−Ag vector, and the more bent disposition of the "$(C_6F_5)_2Pt(\mu\text{-}PPh_2)_2Pd(acac)$" fragment) prompt us to conclude that in **2b** the silver center is connected to the dinuclear Pt/Pd moiety through Pt−Ag and Pd−Ag donor−acceptor bonds of similar strength. This is a surprising result, and at this moment no explanation for the different behaviors of **1a** and **1b** toward $[Ag(PPh_3)]^+$ can be given.

In addition, it has to be pointed out that although we have tried very hard to synthesize complexes with Pd−Ag bonds, in no case were such complexes obtained.[11,17,18] This is presumably because other secondary processes, probably related to the lability of the palladate complexes, took place, preventing the formation of the Pd−Ag-bonded complexes. The Pd−Ag distance observed in **2b** is one of the shortest reported in the literature. Only a few polynuclear Pd/Ag complexes have been reported, but in most cases the Pd−Ag distances are longer than 3 Å,[19−26] and only in two cases are the Pd−Ag distances less than 2.9 Å: $[Pd(H_2O)LAg]^{2+}$ (2.884(2) Å)[25] and $[Mn_2Pd_2Ag(\mu\text{-}Cl)(\mu\text{-}PPh_2)_2(\mu\text{-}dppm)(CO)_8]$ (2.7259(6) and 2.8014(6) Å).[26] In the first case a presumably weak Pd−C(aryl)−Ag interaction is stabilized by peripheral coordination of the silver center to three oxygen atoms of

(16) Yamaguchi, T.; Yamazaki, F.; Ito, T. *J. Am. Chem. Soc.* **2001**, *123*, 743−744.

(17) Falvello, L. R.; Forniés, J.; Martín, A.; Sicilia, V.; Villarroya, P. *Organometallics* **2002**, *21*, 4604−4610.

(18) Usón, R.; Forniés, J.; Tomás, M.; Ara, I.; Casas, J. M.; Martín, A. *J. Chem. Soc., Dalton Trans.* **1991**, 2253−2264.

(19) Yew-Chin-Neo; Vittal, J. J.; Hor, T. S. A. *J. Chem. Soc., Dalton Trans.* **2002**, 337−342.

(20) Ebihara, M.; Tsuchiya, M.; Yamada, M.; Tokoro, K.; Kawamura, T. *Inorg. Chim. Acta* **1995**, *231*, 35−43.

(21) Glaum, M.; Klaui, W.; Skelton, B. W.; White, A. H. *Aust. J. Chem.* **1997**, *50*, 1047−1052.

(22) Usón, R.; Usón, M. A.; Herrero, S. *Inorg. Chem.* **1997**, *36*, 5959−5961.

(23) Ebihara, M.; Tokoro, K.; Maeda, M.; Ogami, M.; Imaeda, K.; Sakurai, K.; Masuda, H.; Kawamura, T. *J. Chem. Soc., Dalton Trans.* **1994**, 3621−3635.

(24) Ardizzoia, G. A.; La Monica, G.; Cenini, S.; Moret, M.; Masciocchi, N. *J. Chem. Soc., Dalton Trans.* **1996**, 1351−1358.

(25) Kickman, J. E.; Loeb, J. J. *Organometallics* **1995**, *14*, 3584−3587.

(26) Liu, Y.; Lee, K. H.; Vittal, J. J.; Hor, T. S. A. *J. Chem. Soc., Dalton Trans.* **2002**, 2747−2751.

the ligand, while in the Mn/Pd/Ag cluster the silver center is exclusively bonded to the four other metal centers.

In **2a**,**b** the planar three-coordination of the silver center is completed by a PPh_3 ligand. The angles around the Ag atom are very different, the Pt(1)−Ag−P(3) angle in **2a** and the analogous Pt−Ag−P(3) angle in **2b** being very broad, 164.8(1) and 166.3(1)°, respectively.

The ^{19}F NMR spectra of **2a**,**b** are very informative. The spectrum of **2a** at room temperature ($CDCl_3$ solution) reflects the solid-state structure. It shows four broad signals: two signals corresponding to *o*-F atoms (1:1 intensity ratio), a signal corresponding to *p*-F atoms (intensity ratio of 1), and a signal for the *m*-F atoms (intensity ratio of 2). This pattern indicates the equivalence of the two C_6F_5 groups and the inequivalence of the halves of each C_6F_5 ring, *m*-F atoms being isochronous. When the spectrum is measured at low temperature, the pattern is the same and the signals are well resolved. Nevertheless, the spectrum of **2b** at room temperature ($CDCl_3$ solution) reveals three broad signals (2:1:2 intensity ratio), which correspond to *o*-F, *p*-F, and *m*-F, respectively, showing that in solution a dynamic process which makes equivalent both halves of each C_6F_5 group is operating. At 213 K, the *o*-F signal is split into two resonances and the pattern is the same that for **2a**. Variable-temperature ^{19}F NMR spectra for **2b** reveal the coalescence of the two *o*-F signals at 278 K. The approximation to Eyring's equation gives a $\Delta G^{\ddagger}$ value of 51 kJ mol^{-1} at the coalescence temperature. The spectrum ($CDCl_3$, room temperature) of **2b** upon addition of **1b** shows signals due to both **2b** and **1b**, indicating that fully dissociative processes which afford **1b** and "$AgPPh_3$" species can be ruled out in $CDCl_3$. The spectra of **2a**,**b** in deuterioacetone at room temperature show two (**2a**, 2:3 intensity ratio, *o*-F and *p* + *m*-F, respectively) or three (**2b**, 2:1:2 intensity ratio, *o*-F, *p*-F, and *m*-F, respectively) signals, and thus, a dynamic process which renders equivalent the halves of each C_6F_5 group is operating for both complexes in deuterioacetone solution. For **2b** the spectra at low temperature reveal that the dynamic process is operating even at 183 K. When the spectrum of **2b** is measured (deuterioacetone, room temperature) with **1b** added, the pattern remains similar; the chemical shifts of all resonances are changed but no signals due to free **1b** are observed. These facts indicate that in deuterioacetone solution a dissociative process which gives **1b** and "$AgPPh_3$" may be operating.

The $^{31}P\{^1H\}$ NMR spectra of **2a**,**b** in $CDCl_3$ show similar patterns at both room and low temperature. The signal due to the PPh_3 group appears as two doublets of triplets by coupling with the $^{107,109}Ag$ atoms (51.8% and 48.2%, respectively) and with the two equivalent P atoms of the PPh_2 groups. From this signal the two $^1J_{Ag-P}$ and the $^3J_{P-P}$ couplings can be calculated. The signal is slightly broadened on the base due to poorly separated platinum satellites. The signal due to the two equivalent PPh_2 groups appears in the high-field region as a singlet with platinum satellites, as expected for the presence of two PPh_2 groups acting as bridging ligands between two metal centers not joined by a metal−metal bond. This singlet is broad, as is usual in all such derivatives in which the PPh_2 groups are trans to C_6F_5 groups, the line width being larger than $^3J_{P-P}$, and so the coupling with PPh_3 cannot be observed in this signal. The $^3J_{P-P}$ coupling observed also indicates that in $CDCl_3$ a dissociative process between $[AgPPh_3]^+$ and $[(C_6F_5)_2Pt(\mu\text{-}PPh_2)_2M(acac)]^-$ does not takes place in any of the complexes.

Moreover, the $^{31}P\{^1H\}$ NMR spectrum of **2a** in deuterioacetone has been recorded. The signal due to the P atom of the PPh_3 group appears as two doublets (two doublets of triplets were observed in $CDCl_3$). Additionally, when the spectrum is recorded with $[Ag(OClO_3)(PPh_3)]$ added, the pattern is the same and no signals due to free $[Ag(OClO_3)(PPh_3)]$ are observed. Both these observations are in agreement with a dissociative process in acetone.

The signals in the ^1H NMR spectra as well as the absorptions in the IR spectra due to the acac ligand of **2a**,**b** are similar to those observed for complexes **1a**,**b**. Experimental details, analytical results, and spectroscopic data for complexes **2a**,**b** are given in the Experimental Section.

The reaction between the homodinuclear palladium complex **1c** and $[Ag(OClO_3)(PPh_3)]$ under similar conditions takes place with decomposition (Scheme 1, path b). The heteronuclear palladium and silver complex, if formed, is not stable enough and the binuclear palladium complex $[(C_6F_5)(PPh_3)Pd(\mu\text{-}PPh_2)_2Pd(acac)]$ (**3**) is identified in the solid by ^1H, ^{19}F, and $^{31}P\{^1H\}$ NMR spectroscopy (see the Experimental Section). As we have previously found, the palladium complex **1c** displays a stronger arylating capability than **1a**,**b**. The reaction process is probably carried out with formation of AgC_6F_5, which decomposes to silver, precluding the formation of a polynuclear palladium and silver derivative. The same process had been observed earlier in the reaction of other palladium complexes with $[Ag(OClO_3)(PPh_3)]$.[11,18]

The behavior of **1a**−**c** toward $[AgPPh_3]^+$ deserves some comment. Obviously, and as we have observed previously, the arylating capability (probably due to the higher lability) of the "$(C_6F_5)_2M(\mu\text{-}PPh_2)_2$" fragment is stronger for the Pd (**1c**) than for the Pt or Pt/Pd (**1a**,**b**) complex. In this respect, differences between **1a** and **1b** are imperceptible, presumably since in this case the Pd center is not bonded to the C_6F_5 groups but to a chelating ligand (acac).

In addition, it is also surprising that despite previous observations[1] which point to the apparent reluctance of the Pd center to engage in Pd−Ag bonds, in these trinuclear complexes a stronger (acac)M−Ag interaction is observed in **2b** (Pd) than in **2a** (Pt), which results not only in clearly shorter M−Ag distances but also in the fact that the booklike structure of the bidentate metalate ligand is more closed in **2b** (Pt, Pd) that in **2a** (Pt, Pt) in order to favor the M−Ag bond.

The reaction of **1a**,**b** with equimolecular amounts of $AgClO_4$ in CH_2Cl_2 at room temperature gives (Scheme 2, path c) yellow solutions from which yellow solids of general formula $[PtMAg(\mu\text{-}PPh_2)_2(C_6F_5)_2(acac)]_x$ (M = Pt, **4a**; M = Pd, **4b**) are obtained. These complexes show similar IR spectra, but unlike complexes **1a**−**c** and **2a**,**b**, the absorptions due to the acac group are different. The IR spectra of **4a**,**b** show two absorptions in the 1570−1590 cm^{-1} region (a broad absorption in this region is observed for **1a**−**c** and **2a**,**b**) while the absorption

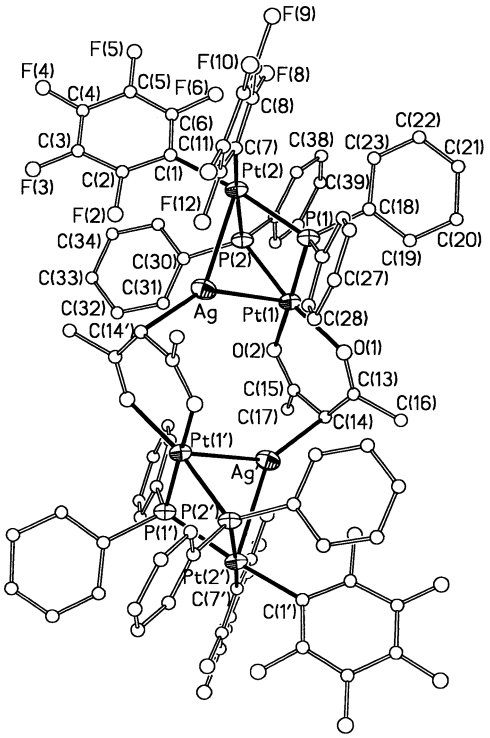

Figure 4. Structure of the complex $[Pt_2Ag(\mu\text{-}PPh_2)_2(C_6F_5)_2(acac)]_2$ (**4a**).

Table 4. Selected Bond Distances (Å) and Angles (deg) for $[Pt_2Ag(\mu\text{-}PPh_2)_2(C_6F_5)_2(acac)]_2\cdot 5.4CHCl_3$ (4a·5.4CHCl$_3$)[a]

Pt(1)−O(2)	2.092(7)	Pt(2)−C(1)	2.051(11)
Pt(1)−Ag	2.875(1)	Pt(2)−P(1)	2.306(3)
Pt(2)−P(2)	2.303(3)	Pt(1)−P(2)	2.269(3)
Ag−C(14′)	2.318(11)	Pt(2)−C(7)	2.063(11)
Pt(1)−P(1)	2.267(3)	Pt(2)−Ag	2.864(1)
O(2)−Pt(1)−O(1)	89.2(3)	O(2)−Pt(1)−P(1)	171.5(2)
O(1)−Pt(1)−P(1)	96.4(2)	O(2)−Pt(1)−P(2)	96.1(2)
O(1)−Pt(1)−P(2)	171.2(2)	P(1)−Pt(1)−P(2)	77.58(10)
C(1)−Pt(2)−C(7)	90.2(4)	C(1)−Pt(2)−P(2)	95.8(3)
C(7)−Pt(2)−P(2)	173.1(3)	C(1)−Pt(2)−P(1)	171.5(3)
C(7)−Pt(2)−P(1)	97.7(3)	P(2)−Pt(2)−P(1)	76.13(10)
C(14′)−Ag−Pt(2)	140.3(3)	C(14′)−Ag−Pt(1)	145.1(3)
Pt(2)−Ag−Pt(1)	74.61(3)	Pt(1)−P(1)−Pt(2)	99.03(11)
Pt(1)−P(2)−Pt(2)	99.07(11)		

[a] Symmetry transformations used to generate equivalent (primed) atoms: $1/2 - x$, $5/2 - y$, $-z$.

observed at approximately 1510−1520 cm^{-1} for **1a**−**c** and **2a**,**b** is not observed. Moreover, new absorptions in the 850−840 cm^{-1} region are observed for **4a**,**b**. Absorptions in this region have been observed for complexes which contain the acac group coordinated through the C$^{\gamma}$ atom.[13] These data seem to indicate that for complexes **4a**,**b** the coordination mode of the acac ligands is different than in **1a**−**c** and **2a**,**b**. The structure of **4a** has been elucidated by an X-ray diffraction study (see Figure 4). Selected bond distances and angles are listed in Table 4. The molecular formula of the complex is $[Pt_2Ag(C_6F_5)_2(PPh_2)_2(acac)]_2$. It has an inversion center, and therefore, the geometries of the "$Pt_2Ag(C_6F_5)_2(PPh_2)_2(acac)$" halves are identical. **4a** is a hexanuclear complex, which, for description purposes, can be regarded as two "$Pt_2(acac)(C_6F_5)_2(\mu\text{-}PPh_2)_2$" fragments joined by two silver atoms. In the former the dihedral angle between the two platinum square-planar environments is 25.5(1)° and the Pt(1)−Pt(2) distance is 3.478(1) Å, precluding the existence of a Pt−Pt bond. The two Pt−Ag bonds are of virtually the same length (distances are Pt(1)−Ag = 2.875(1) Å and Pt(2)−Ag = 2.864(1) Å). In this case, the angles formed by the Pt−Ag bond lines and the perpendicular to the best square planes are similar, 27.3(1)° for Pt(1) and 21.8(1)° for Pt(2). All these parameters indicate that, in this complex, both Pt−Ag bonds are of similar strength.

The presence of ClO_4^- in the reaction could have led to the formation of a trinuclear complex, similar to **2a**, with the perchlorate anion coordinated to the silver center. Despite the low coordination capacity of the perchlorate anion, complexes containing the Ag−OClO$_3$ moiety are well-known.[17,27,28] Nevertheless, in **4a** the Ag atoms complete their coordination environment by forming a bond with the C$^{\gamma}$ (C(14′)) carbon atom of the acac ligand. The Ag−C(14′) distance is 2.318(11) Å, which is slightly longer than those found in the anion $[Pd_2Ag(acac)_2(C_6F_5)_4]^-$, which also shows the silver atom bonded to the C$^{\gamma}$ carbon atom of the acac ligand (the Ag−C distance is 2.237(7) Å).[12] For **4a**, the Ag atom and the three atoms bonded to it are coplanar, and the Pt−Ag−C(14′) angles are similar (145.1(3)° for Pt(1) and 140.3(3)° for Pt(2)) and very different from the Pt(1)−Ag−Pt(2) angle.

Due to the formation of the Ag−C(14′) bond, the acac ligand loses its planarity. Thus, while Pt(1), O(1), O(2), C(13), and C(15) are virtually in the same plane, the methyl carbon atoms C(16) and C(17) deviate ca. 0.34 Å in the opposite direction to the Ag atom, and the C(14) atom approaches the Ag atom and deviates 0.21 Å from this plane. Nevertheless, the distortion of the acac ligand in **4a** from the noncoordinated configuration, as found in **2a**,**b** (see above), is less pronounced than that described for $[NBu_4][Pd_2Ag(acac)_2(C_6F_5)_4]$.[12] This fact could be explained by taking into account that for this complex the silver atom is two-coordinated, whereas in **4a** it is three-coordinated, and thus the strength of the Ag−C interactions is likely to be reduced, as reflected in the longer bond length.

The $^{31}P\{^1H\}$ NMR (CD_2Cl_2 or $CDCl_3$ solution) spectroscopic data of **4a**,**b** are analogous to those of the starting material, as expected. The ^{19}F NMR spectra of **4a**,**b** (CD_2Cl_2 or $CDCl_3$ solution, room temperature) show the same pattern: five signals of the same intensity. Two of them at lower field and with platinum satellites are assigned to the *o*-F atoms, and three signals at higher field are due to *m*- and *p*-F atoms. These spectra indicate the equivalence of the four C_6F_5 groups and the inequivalence of both halves of each C_6F_5 ring. The ^1H NMR (CD_2Cl_2 or $CDCl_3$ solution) spectra show in both cases a singlet for the equivalent CH_3 groups of the acac ligand. The C$^{\gamma}$H protons appear as a broad signal centered at 5.9 ppm for complex **4a** and as a doublet (9 Hz) centered at 5.7 ppm for **4b**. This doublet can be attributed to the coupling with the $^{107,109}Ag$ nuclei. Since the difference of magnetogyric ratios of ^{107}Ag and ^{109}Ag is small ($\gamma(^{107}Ag)/\gamma(^{109}Ag) = 1.15$), it is assumed that $^2J(^{107}Ag-H) \approx {}^2J(^{109}Ag-H) \approx 9$ Hz. Similar coupling constants of $^2J_{Ag-H}$ have been re-

(27) Falvello, L. R.; Forniés, J.; Fortuño, C.; Durán, F.; Martín, A. *Organometallics* **2002**, *21*, 2226−2234.
(28) Ara, I.; Forniés, J.; Gómez, J.; Lalinde, E.; Merino, R. I.; Moreno, M. T. *Inorg. Chem. Commun.* **1999**, *2*, 62−65.

ported.[29] In complex **4a** the $^2J_{Ag-H}$ value is small and the coupling is not resolved. All these data are in accordance with the solid-state structure of **4a**.

Nevertheless, the ^1H and ^{19}F NMR spectra measured in deuterioacetone are different. The ^{19}F NMR spectra of **4a**,**b** in deuterioacetone show one signal with platinum satellites for the *o*-F atoms and a signal for the *m*- + *p*-F atoms (intensity ratio 2:3), indicating the equivalence of both halves in each C_6F_5 ring. The ^1H NMR spectra in deuterioacetone show the signal due to the $C^{\gamma}H$ protons as a sharp singlet. Moreover, the spectra of **4b** have been measured at 183 K and they are the same as those at room temperature. The ^{19}F and ^1H spectra of both **4a** and **4b** undergo a change upon addition of the starting materials **1a** and **1b**, respectively. The pattern remains similar, but the chemical shifts of resonances have changed, and no signals due to **1a** or **1b** are observed. All these facts are in agreement with a dissociative process involving the starting material; i.e., in the donor solvent both the Pt−Ag and Ag−C bonds are cleaved, leading to formation of the ionic species $[(C_6F_5)_2Pt(\mu\text{-}PPh_2)_2Pt(acac)]^-$ and $[Ag(acetone)_x]^+$.

The molar conductivities of complexes **2a**,**b** and **4a**,**b** in dichloromethane and in acetone (see the Experimental Section) are in agreement with the dissociative processes proposed from the NMR data.

The reaction of $[NBu_4][(C_6F_5)_2Pt(\mu\text{-}PPh_2)_2Pt(acac)]$ (**1a**) and $AgClO_4$ in a 1:2 molar ratio (CH_2Cl_2, room temperature) in an attempt to form a derivative with dicoordinated silver only gives complex **4a**. On the other hand, the reaction in a 2:1 molar ratio intended to form a pentanuclear derivative with two $[(C_6F_5)_2Pt(\mu\text{-}PPh_2)_2Pt(acac)]^-$ fragments bonded to one silver center gives a mixture, which contains **4a** and the platinum starting material. Both facts point to the stability of the hexanuclear derivative containing three-coordinated silver.

The hexanuclear derivative **4a** reacts, as expected, with PPh_3 (1:2 molar ratio), yielding the trinuclear complex $[Pt_2Ag(\mu\text{-}PPh_2)_2(C_6F_5)_2(acac)(PPh_3)]$ (**2a**), through the selective breaking of the C−Ag bonds.

As previously observed, **1c** does not react with $AgClO_4$ (CH_2Cl_2) to form a similar hexanuclear derivative, but decomposition and formation of Ag(0) results.

Concluding Remarks

The reaction of $[NBu_4][(C_6F_5)_2Pt(\mu\text{-}PPh_2)_2M(acac)]$ with $[Ag(OClO_3)(PPh_3)]$ and $AgClO_4$ gives tri- or hexanuclear complexes in which the metalate fragments act either as bidentate or as tridentate ligands. The donor centers Pt and Pd in the former and Pt, Pd, and C (of the acac group) in the latter are bonded to the silver fragment.

This result is in sharp contrast with the behavior of $[NBu_4]_2[(C_6F_5)_2Pt(\mu\text{-}PPh_2)_2Pt(C_6F_5)_2]$, which with $AgClO_4$ produces the oxidation to the Pt(III) derivative $[(C_6F_5)_2Pt(\mu\text{-}PPh_2)_2Pt(C_6F_5)_2]$ and formation of Ag^0.

The formation of **2b**, which contains Pt−Ag and Pd−Ag donor−acceptor bonds, seems to indicate that the impossibility of synthesizing complexes with Pd−Ag bonds through the reaction of anionic palladate complexes and silver salts could well be related to the lability of the palladate substrate, which transfers R groups to the silver and thereby prevents the formation of the Pd−Ag bonds. The substrate **1b**, in which the Pd center is not bonded to C_6F_5 groups, does not produce such transference and forms the Pd−Ag bond. Although it seems reasonable to think that the formation of the Pd−Ag bond is additionally favored by the chelate effect of the metallo ligand, it is rather surprising that such an effect is not operating in complex **2a**, which does not display two Pt−Ag bonds. We have not been able to find a plausible explanation for this fact.

Finally, it is not surprising that **1c** is not able to produce complexes with Pd−Ag bonds in any case, since arylating processes, which militate against the formation of Pd−Ag bonds, are operating in the reaction of **1c** with Ag^+ or $[Ag(PPh_3)]^+$, because one of the palladium centers is bonded to two C_6F_5 groups.

Experimental Section

General Comments. Literature methods were used to prepare the starting material $[NBu_4]_2[(C_6F_5)_2M(\mu\text{-}PPh_2)_2M'(\mu\text{-}Cl)_2M'(\mu\text{-}PPh_2)_2M(C_6F_5)_2]$.[30] C, H, and N analyses and IR and NMR spectra were performed as described elsewhere.[31] Molar conductances were carried out on a Philips PW9509 conductimeter in acetone and dichloromethane solutions (5×10^{-4} M).

Caution! Perchlorate salts of metal complexes with organic ligands are potentially explosive. Only small amounts of material should be prepared, and these should be handled with great caution.

Synthesis of $[NBu_4][(C_6F_5)_2M(\mu\text{-}PPh_2)_2M'(acac\text{-}O,O')]$. M = M′ = Pt (1a). To a solution of $[NBu_4]_2[(C_6F_5)_2Pt(\mu\text{-}PPh_2)_2Pt(\mu\text{-}Cl)_2Pt(\mu\text{-}PPh_2)_2Pt(C_6F_5)_2]$ (0.495 g, 0.180 mmol) in CH_2Cl_2 (25 mL) was added Tl(acac) (0.109 g, 0.360 mmol). The mixture was stirred for 4 h, and then the solid (TlCl) was filtered off. The resulting solution was evaporated to ca. 2 mL, and ^{i}PrOH (15 mL) was added. The white solid obtained, **1a**, was filtered off, washed with ^{i}PrOH (3 × 1 mL), and dried under vacuum (0.449 g, 87%). Anal. Found (calcd) for $C_{57}F_{10}H_{63}NO_2P_2Pt_2$: C, 47.7 (47.7); H, 4.8 (4.4); N, 1.1 (1.0). IR (cm^{-1}): 781 and 773 (X-sensitive C_6F_5); 1579 (broad) and 1519 (ν(C═C), ν(C═O) acac). Λ_M = 71 (acetone) Ω^{-1} cm^2 mol^{-1}. ^1H NMR ([^2H]acetone, δ): 5.2 (1H, C$^{\gamma}H$, acac), 1.8 (6H, CH_3, acac) ppm. ^{19}F NMR ([^2H]acetone, δ): −113.9 (4 *o*-F, $^3J_{Pt,F}$ = 297 Hz), −166.2 (4 *m*-F), −167.1 (2 *p*-F) ppm. $^{31}P\{^1H\}$ NMR ([^2H]acetone, δ): −144.6 ($^1J_{Pt,P}$ = 2641 and 1912 Hz) ppm.

M = Pt, M′ = Pd (1b). Complex **1b** was prepared similarly from $[NBu_4]_2[(C_6F_5)_2Pt(\mu\text{-}PPh_2)_2Pd(\mu\text{-}Cl)_2Pd(\mu\text{-}PPh_2)_2Pt(C_6F_5)_2]$ (0.500 g, 0.195 mmol) and Tl(acac) (0.118 g, 0.389 mmol). **1b** was obtained as a yellow solid (0.368 g, 70%). Anal. Found (calcd) for $C_{57}F_{10}H_{63}NO_2P_2PdPt$: C, 50.8 (50.8); H, 4.8 (4.7); N, 1.1 (1.0). IR (cm^{-1}): 782 and 773 (X-sensitive C_6F_5); 1582 (broad) and 1512 (ν(C═C), ν(C═O) acac). Λ_M = 96 Ω^{-1} cm^2 mol^{-1} (acetone). ^1H NMR ([^2H]acetone, δ): 5.2 (1H, C$^{\gamma}H$, acac), 1.7 (6H, CH_3, acac) ppm. ^{19}F NMR ([^2H]acetone, δ): −114.0 (4 *o*-F, $^3J_{Pt,F}$ = 321 Hz), −166.2 (4 *m*-F), −166.9 (2 *p*-F) ppm. $^{31}P\{^1H\}$ NMR ([^2H]acetone, δ): −134.2 ($^1J_{Pt,P}$ = 1785 Hz) ppm.

M = M′ = Pd (1c). Complex **1c** was prepared in a manner similar to that for **1a** from $[NBu_4]_2[(C_6F_5)_2Pd(\mu\text{-}PPh_2)_2Pd(\mu\text{-}Cl)_2Pd(\mu\text{-}PPh_2)_2Pt(C_6F_5)_2]$ (0.350 g, 0.146 mmol) and Tl(acac) (0.089 g, 0.293 mmol). **1c** was obtained as a yellow solid (0.290 g, 78%). Anal. Found (calcd) for $C_{57}F_{10}H_{63}NO_2P_2Pd_2$: C, 53.9 (54.4); H, 5.1 (5.0); N, 1.0 (1.1). IR (cm^{-1}): 775 and 769 (X-

(29) Wang, S.; Fackler, J. P. J.; Carlson, T. F. *Organometallics* **1990**, *9*, 1973−1975.

(30) Forniés, J.; Fortuño, C.; Navarro, R.; Martínez, F.; Welch, A. J. *J. Organomet. Chem.* **1990**, *394*, 643−658.

(31) Alonso, E.; Forniés, J.; Fortuño, C.; Martín, A.; Orpen, A. G. *Organometallics* **2000**, *19*, 2690−2697.

Table 5. Crystal Data and Structure Refinement Details for [NBu$_4$][PtPd(μ-PPh$_2$)$_2$(C$_6$F$_5$)$_2$(acac)]·Me$_2$CO (1b·Me$_2$CO), [Pt$_2$Ag(μ-PPh$_2$)$_2$(C$_6$F$_5$)$_2$(acac)(PPh$_3$)]·CHCl$_3$ (2a·CHCl$_3$), [PtPdAg(μ-PPh$_2$)$_2$(C$_6$F$_5$)$_2$(acac)(PPh$_3$)]·2.5CH$_2$Cl$_2$ (2b·2.5CH$_2$Cl$_2$), and [Pt$_2$Ag(μ-PPh$_2$)$_2$(C$_6$F$_5$)$_2$(acac)]$_2$·5.4CHCl$_3$ (4a·5.4CHCl$_3$)

	1b·Me$_2$CO	**2a**·CHCl$_3$	**2b**·2.5CH$_2$Cl$_2$	**4a**·5.4CHCl$_3$
empirical formula	$C_{57}H_{82}F_{10}NO_2P_2PdP$·Me$_2$CO	$C_{59}H_{42}AgF_{10}O_2P_3Pt_2$·CHCl$_3$	$C_{59}H_{41}F_{10}O_2P_3AgPdPt$·2.5CH$_2Cl_2$	$C_{82}H_{52}F_{20}O_4P_4Ag_2Pt_4$·5.4CHCl$_3$
unit cell dimens				
a (Å)	22.9957(13)	13.261(5)	12.3204(18)	30.086(5)
b (Å)	12.0462(6)	22.962(7)	23.828(4)	14.088(2)
c (Å)	21.6125(12)	20.048(7)	20.266(3)	26.994(4)
β (deg)	100.2130(10)	96.63(3)	93.780(3)	106.892(8)
V (Å^3), *Z*	5892.0(6), 4	6064(4), 4	5936.5(15), 4	10948(3), 4
wavelength (Å)	0.710 73			
temp (K)	100(1)	293(1)	100(1)	173(1)
radiation	graphite monochromated Mo Kα			
cryst syst	monoclinic			
space group	$P2_1/c$	$P2_1/n$	$P2_1/n$	$C2/c$
cryst dimens (mm)	0.45 × 0.44 × 0.40	0.50 × 0.40 × 0.30	0.41 × 0.31 × 0.29	0.50 × 0.45 × 0.40
abs coeff (mm^{-1})	2.807	5.206	3.313	5.975
transmissn factors	1.000−0.875	0.601−0.481	1.000−0.805	0.943−0.560
abs cor	SADABS[33]	Ψ scans	SADABS[33]	SADABS[33]
diffractometer	Bruker SMART	Siemens P3m	Bruker SMART	Siemens SMART
2θ range for data collecn (deg)	0.90−25.03	1.75−25.00	1.32−25.03	1.41−23.26
no. of rflns collected	31 413	11 181	34 674	22 693
no. of indep rflns	10 386 (R(int) = 0.0246)	10 688 (R(int) = 0.0302)	10 483 (R(int) = 0.0350)	7814 (R(int) = 0.0532)
refinement method	full-matrix least-squares on F^2			
goodness of fit on F^2	1.040	1.253	1.011	1.514
final R indices ($I > 2\sigma(I)$)[a]	R1 = 0.0230	R1 = 0.0413	R1 = 0.0412	R1 = 0.0512
	wR2 = 0.0524	wR2 = 0.0968	wR2 = 0.1288	wR2 = 0.1287
R indices (all data)	R1 = 0.0284	R1 = 0.0626	R1 = 0.0504	R1 = 0.0688
	wR2 = 0.0602	wR2 = 0.1146	wR2 = 0.1334	wR2 = 0.1418

[a] R1 = $\sum(|F_o| - |F_c|)/\sum|F_o|$; wR2 = $[\sum w(F_o^2 - F_c^2)^2/\sum w(F_c^2)^2]^{0.5}$.

sensitive C$_6$F$_5$); 1581 and 1512 (ν(C═C), ν(C═O) acac). Λ_M = 84 Ω^{-1} cm^2 mol^{-1} (acetone). ^{1}H NMR ([^{2}H]acetone, δ): 5.1 (1H, C$^\gamma$*H*, acac), 1.7 (6H, C*H*$_3$, acac) ppm. ^{19}F NMR ([^{2}H]acetone, δ): −110.9 (4 *o*-F, Hz), −165.3 (4 *m*-F), −165.9 (2 *p*-F) ppm. ^{31}P{^{1}H} NMR ([^{2}H]acetone, δ): −115.6 ppm.

Preparation of [PtMAg(μ-PPh$_2$)$_2$(C$_6$F$_5$)$_2$(acac)(PPh$_3$)]. M = Pt (2a). To a solution of **1a** (0.125 g, 0.087 mmol) in 10 mL of CH$_2$Cl$_2$ was added [Ag(OClO$_3$)(PPh$_3$)] (0.041 g, 0.087 mmol), and the solution was stirred at room temperature for 2 h with exclusion of light. The yellow solution was evaporated to dryness, and Et$_2$O (10 mL) was added. The insoluble NBu$_4$ClO$_4$ was separated, the solution was evaporated to 2 mL, *n*-hexane (10 mL) was added, and the mixture was stirred vigorously, giving **2a** (0.095 g, 70%) as a yellow solid. Anal. Found (calcd) for AgC$_{59}$F$_{10}$H$_{42}$O$_2$P$_3$Pt$_2$: C, 45.5 (45.3); H, 2.6 (2.7). IR (cm^{-1}): 787 and 780 (X-sensitive C$_6$F$_5$); 1560 and 1520 (ν(C═C), ν(C═O) acac). Λ_M = 1 Ω^{-1} cm^2 mol^{-1} (CH$_2$Cl$_2$), 64 Ω^{-1} cm^2 mol^{-1} (acetone). ^{1}H NMR (CDCl$_3$, 218 K, δ): 5.6 (1H, C$^\gamma$*H*, acac), 2.0 (6H, C*H*$_3$, acac) ppm. ^{19}F NMR (CDCl$_3$, 293 K, δ): −115.9 (2 *o*-F, $^3J_{Pt,F}$ = 473 Hz), −118.3 (2 *o*-F, $^3J_{Pt,F} \approx$ 300 Hz), −164.1 (2 *p*-F), −164.6 (4 *m*-F) ppm. ^{19}F NMR (CDCl$_3$, 218 K, δ): −115.9 (2 *o*-F, $^3J_{Pt,F}$ = 480 Hz), −118.1 (2 *o*-F, $^3J_{Pt,F}$ = 254 Hz), −163.0 (2 *p*-F), −163.6 (4 *m*-F) ppm. ^{31}P{^{1}H} NMR (CDCl$_3$, 218 K, δ): −136.3 (*P*Ph$_2$, $^1J_{Pt,P}$ = 2269 and 1455 Hz), 6.1 (*P*Ph$_3$, $^1J_{Ag,P}$ = 764 (^{109}Ag) and 662 (^{107}Ag) Hz, $^3J_{P,P}$ = 29 Hz) ppm.

M = Pd (2b). Complex **2b** was prepared similarly from **1b** (0.100 g, 0.074 mmol) and [Ag(OClO$_3$)(PPh$_3$)] (0.035 g, 0.074 mmol); yield 0.082 g, 75%. Anal. Found (calcd) for AgC$_{59}$F$_{10}$H$_{42}$O$_2$P$_3$PdPt: C, 48.3 (48.0); H, 2.95 (2.9). IR (cm^{-1}): 787 and 780 (X-sensitive C$_6$F$_5$); 1577 and 1514 (ν(C═C), ν(C═O) acac). Λ_M = 1 Ω^{-1} cm^2 mol^{-1} (CH$_2$Cl$_2$), 39 Ω^{-1} cm^2 mol^{-1} (acetone). ^{1}H NMR (CDCl$_3$, 218 K, δ): 5.4 (1H, C$^\gamma$*H*, acac), 1.8 (6H, C*H*$_3$, acac) ppm. ^{19}F NMR (CDCl$_3$, 293 K, δ): −117.0 (4 *o*-F, the signal is broad and $^3J_{Pt,F}$ cannot be measured), −163.2 (2 *p*-F), −163.8 (4 *m*-F) ppm. ^{19}F NMR (CDCl$_3$, 218 K, δ): −116.6 (2 *o*-F, $^3J_{Pt,F}$ = 494 Hz), −118.5 (2 *o*-F, $^3J_{Pt,F}$ = 245 Hz), −162.6 (2 *p*-F), −163.3 (4 *m*-F) ppm. ^{31}P{^{1}H} NMR (CDCl$_3$, 218 K, δ): −122.4 (*P*Ph$_2$, $^1J_{Pt,P}$ = 1367 Hz), 9.3 (*P*Ph$_3$, $^1J_{Ag,P}$ = 772 (^{109}Ag) and 649 (^{107}Ag) Hz, $^3J_{P,P}$ = 27 Hz) ppm.

Reaction of 1c with [Ag(OClO$_3$)(PPh$_3$)]. Following a procedure similar to that for **2a**, the reaction of **1c** (0.100 g, 0.079 mmol) and an equimolecular amount of [Ag(OClO$_3$)(PPh$_3$)] (0.037 g, 0.079 mmol) gives a brown solid in which [(C$_6$F$_5$)(PPh$_3$)Pd(μ-PPh$_2$)$_2$Pd(acac)] (**3**) is identified. ^{1}H NMR (CDCl$_3$, 293 K, δ): 5.2 (1H, C$^\gamma$*H*, acac), 1.7 (3H, C*H*$_3$, acac), 1.6 (3H, C*H*$_3$, acac) ppm. ^{19}F NMR (CDCl$_3$, 293 K, δ): −115.1 (2 *o*-F), −163.4 (3 *m*- + *p*-F) ppm. ^{31}P{^{1}H} NMR (CDCl$_3$, 293 K, δ): 23.3 (d, *P*Ph$_3$, $^2J_{(P,P)trans}$ = 354 Hz), −97.3 (dd, *P*Ph$_2$, $^2J_{(P,P)trans}$ = 354 Hz, $^2J_{(P,P)cis}$ = 153 Hz) ppm, −114.0 (d, *P*Ph$_2$, $^2J_{(P,P)cis}$ = 153 Hz) ppm.

Preparation of [Pt$_2$M$_2$Ag$_2$(μ-PPh$_2$)$_4$(C$_6$F$_5$)$_4$(acac)$_2$]. M = Pt (4a). To a colorless solution of **1a** (0.100 g, 0.069 mmol) in CH$_2$Cl$_2$ (25 mL) was added AgClO$_4$ (0.029 g, 0.138 mmol), and the mixture was stirred at room temperature for 1 h and then filtered. The yellow solution was evaporated to 1.5 mL and left in the freezer for 3 h. A yellow solid of **4a** crystallized, which was filtered off, washed with cold CH$_2$Cl$_2$ (2 × 0.5 mL), and dried under vacuum; yield 0.072 g, 80%. Anal. Found (calcd) for Ag$_2$C$_{82}$F$_{20}$H$_{54}$O$_4$P$_4$Pt$_4$: C, 38.0 (37.8); H, 2.3 (2.1). IR (cm^{-1}): 788 and 781 (X-sensitive C$_6$F$_5$); 1574 and 1570 (ν(C═C), ν(C═O) acac); 851 broad (acac). Λ_M = 4 Ω^{-1} cm^2 mol^{-1} (CH$_2$Cl$_2$), 61 Ω^{-1} cm^2 mol^{-1} (acetone). ^{1}H NMR (CD$_2$Cl$_2$, 293 K, δ): 5.9 (2H, C$^\gamma$*H*, acac), 2.1 (12H, C*H*$_3$, acac) ppm. ^{19}F NMR (CD$_2$Cl$_2$, 293 K, δ): −115.5 (4 *o*-F, $^3J_{Pt,F}$ = 479 Hz), −117.3 (4 *o*-F, $^3J_{Pt,F}$ = 271 Hz), −162.6 (4 *p*-F), −163.3 (4 *m*-F), −163.7 (4 *m*-F) ppm. ^{31}P{^{1}H} NMR (CD$_2$Cl$_2$, 293 K, δ): −121.2 ($^1J_{Pt,P}$ = 2154 and 1523 Hz) ppm.

M = Pd (4b). Complex **4b** was prepared similarly from **1b** (0.102 g, 0.076 mmol) in CH$_2$Cl$_2$ (40 mL) and AgClO$_4$ (0.018 g, 0.087 mmol). From the dark yellow solution **4b** crystallized as a yellow solid; yield 0.056 g, 61%. Anal. Found (calcd) for Ag$_2$C$_{82}$F$_{20}$H$_{54}$O$_4$P$_4$Pd$_2$Pt$_2$: C, 40.8 (40.6); H, 2.4 (2.2). IR (cm^{-1}): 790 and 782 (X-sensitive C$_6$F$_5$); 1591 and 1581 (ν(C═C),

ν(C═O) acac); 847 and 837 (acac). $\Lambda_M = 2\ \Omega^{-1}\ cm^2\ mol^{-1}$ (CH_2Cl_2), 89 $\Omega^{-1}\ cm^2\ mol^{-1}$ (acetone). ^{1}H NMR ($CDCl_3$, 293 K, δ): 5.7 (2H, $^2J_{^{107}Ag,H} \approx {}^2J_{^{109}Ag,H} \approx 9$ Hz, C$^{\gamma}H$, acac), 2.0 (12H, CH_3, acac) ppm. ^{19}F NMR ($CDCl_3$, 293 K, δ): −117.0 (4 *o*-F, $^3J_{Pt,F} =$ 499 Hz), −118.1 (4 *o*-F, $^3J_{Pt,F} = 276$ Hz), −162.1 (4 *p*-F), −163.0 (4 *m*-F), −163.9 (4 *m*-F) ppm. ^{31}P{^{1}H} NMR ($CDCl_3$, 293 K, δ): −105.3 ($^1J_{Pt,P} = 1383$ Hz) ppm.

Reaction of 4a with PPh_3. To a yellow solution of **4a** (0.050 g, 0.019 mmol) in 10 mL of CH_2Cl_2 was added PPh_3 (0.010 g, 0.038 mmol), and the solution was stirred at room temperature for 30 min with exclusion of light. The solution was evaporated almost to dryness, *n*-hexane (10 mL) was added, and the mixture was stirred vigorously, giving **2a** (0.045 g, 76%).

Crystal Structure Analyses of $[NBu_4][PtPd(\mu\text{-}PPh_2)_2(C_6F_5)_2(acac)]\cdot Me_2CO$ (1b·Me_2CO), $[Pt_2Ag(\mu\text{-}PPh_2)_2(C_6F_5)_2(acac)(PPh_3)]\cdot CHCl_3$ (2a·$CHCl_3$), $[PtPdAg(\mu\text{-}PPh_2)_2(C_6F_5)_2(acac)(PPh_3)]\cdot 2.5CH_2Cl_2$ (2b·$2.5CH_2Cl_2$), and $[Pt_2Ag(\mu\text{-}PPh_2)_2(C_6F_5)_2(acac)]_2\cdot 5.4CHCl_3$ (4a·$5.4CHCl_3$). Crystal data and other details of the structure analysis are presented in Table 5. Suitable crystals of **1a**, **2a**, **2b**, and **4a** were obtained by slow diffusion of *n*-hexane into an acetone (**1b**), $CHCl_3$ (**2a** and **4a**), or CH_2Cl_2 (**2b**) solution of the complex. Crystals were mounted at the end of a glass fiber. For **1b**, unit cell dimensions were initially determined from the positions of 729 reflections in 90 intensity frames measured at 0.3° intervals in ω and subsequently refined on the basis of positions of 7422 reflections from the main data set. An absorption correction was applied on the basis of 2942 symmetry-equivalent reflection intensities. For **2a**, unit cell dimensions were determined from 50 centered reflections in the range $15.0 < 2\theta < 28.5°$. An absorption correction was applied on the basis of 504 azimuthal scan data. For **2b**, unit cell dimensions were initially determined from the positions of 408 reflections in 90 intensity frames measured at 0.3° intervals in ω and subsequently refined on the basis of positions of 6552 reflections from the main data set. An absorption correction was applied on the basis of 4063 symmetry-equivalent reflection intensities. For **4a**, unit cell dimensions were initially determined from the positions of 282 reflections in 90 intensity frames measured at 0.3° intervals in ω and subsequently refined on the basis of positions of 5556 reflections from the main data set. An absorption correction was applied on the basis of 15505 symmetry-equivalent data. Lorentz and polarization corrections were applied for all the structures.

The structures were solved by Patterson and Fourier methods. All refinements were carried out using the program SHELXL-93.[32] All non-hydrogen atoms were assigned anisotropic displacement parameters and refined without positional constraints, except as noted below. All hydrogen atoms were constrained to idealized geometries and assigned isotropic displacement parameters 1.2 times the U_{iso} value of their attached carbon atoms (1.5 times for methyl hydrogen atoms). For **2b**, constraints in the C−Cl distances were applied for the half-occupancy dichloromethane solvent molecule. For **4a**, restraints in the bond distances for the solvent molecules were applied. Full-matrix least-squares refinement of these models against F^2 converged to the final residual indices given in Table 4. Final difference electron density maps showed no features above 1 e/Å^3 (maximum/minimum 0.90/−0.64 e/Å^3) for **1b**, no features above 1 e/Å^3 (maximum/minimum 0.81/−0.77 e/Å^3) for **2a**, 41 features above 1 e/Å^3 (maximum/minimum 2.97/−2.90 e/Å^3, the largest of which lie close to the heavy and solvent atoms for **2b** (these latter features are consistent with the presence of systematic errors in the intensity data). Variations in the integration procedures—changing integration "shoebox" sizes etc.—and in the absorption correction methods did not improve the R(int) or final wR2 values or reduce the size of features in the final difference map. In addition, the molecular geometry determined remained essentially invariant throughout). In **4a**·$5.4CHCl_3$ there is one feature above 1 e/Å^3 (maximum/minimum 1.25/−1.40 e/Å^3) close to one of the platinum atoms.

Acknowledgment. We wish to thank the Ministerio de Ciencia Tecnología y Fondos FEDER (Project BQU-2002-03997-C02-02). E.A. and A.M. acknowledge the Diputación General de Aragón and the GES (Spain), respectively, for their grants.

Supporting Information Available: Further details of the structure determinations of **1b**·Me_2CO, **2a**·$CHCl_3$, **2b**·$2.5CH_2Cl_2$, and **4a**·$5.4CHCl_3$, including tables of atomic coordinates, bond distances and angles, and thermal parameters; these data are also available as CIF files. This material is available free of charge via the Internet at http://pubs.acs.org.

OM034047F

(32) Sheldrick, G. M. SHELXL-93, a Program for Crystal Structure Determination; University of Gottingen, Gottingen, Germany, 1993.
(33) Sheldrick, G. M. SADABS Empirical Absorption Program; University of Gottingen, Gottingen, Germany, 1996.
(34) Alonso, E.; Forniés, J.; Fortuño, C.; Martín, A.; Orpen, A. G. *Organometallics* **2003**, *22*, 2723−2728.